Electronic Supplementary Material (ESI) for Physical Chemistry Chemical Physics.

Lithium-ion battery degradation: how to model it Supplementary Information

Simon E. J. O'Kane[1,6,a], Weilong Ai[2,6,b], Ganesh Madabattula[1,6,c], Diego Alonso Alvarez[3,6], Robert Timms[4,6], Valentin Sulzer[5,6], Jacqueline Sophie Edge[1,6], Billy Wu[2,6], Gregory J. Offer[1,6], Monica Marinescu[1,6]

[1]Department of Mechanical Engineering, Imperial College London, UK
[2]Dyson School of Design Engineering, Imperial College London, UK
[3]Research Computing Service, ICT, Imperial College London, UK
[4]Mathematical Institute, University of Oxford, UK
[5]Department of Mechanical Engineering, Carnegie Mellon University, USA
[6]The Faraday Institution, UK

[a]Email: s.okane@imperial.ac.uk
[b]Current address: School of Civil Engineering, Southeast University, PR China
[c]Current address: BritishVolt Ltd., UK

23rd February 2022

DFN model equations

The basic DFN model equations are listed in Table S1. The notation is the same as that used by O'Kane *et* al.[1], with two changes: N_{sr} now denotes side reactions in general as opposed to Li plating specifically, and the voltage drop η_{SEI} due to the SEI resistance has been added to the Butler-Volmer equation.

Electrode parameters

The open-circuit potential curves $U_{\pm}(c_{\mathrm{s}}^{*})$ were measured by Chen *et* al.[2] at 25 °C and are replotted in Fig. S1. For both electrodes, the three-electrode cell measurements were used. Chen *et* al.found that the graphite+SiO_{x} negative electrode showed significant hysteresis; the discharge branch of the OCP is used in the model, as in Chen *et* al.'s own PyBaMM model.

Variable	Equation
$\phi_{\mathrm{s}}(x,t)$	$\sigma_{\pm}\dfrac{\partial^2\phi_{\mathrm{s}}}{\partial x^2} = j_{\mathrm{tot}}$
$\phi_{\mathrm{e}}(x,t)$	$-\kappa_{\mathrm{eff}}(c_{\mathrm{e}},T)\dfrac{\partial^2\phi_{\mathrm{e}}}{\partial x^2} + \dfrac{2RT}{F}\kappa_{\mathrm{eff}}(c_{\mathrm{e}},T)(1-t^+)\dfrac{\partial^2 \ln c_{\mathrm{e}}}{\partial x^2} = j_{\mathrm{tot}}$
$c_{\mathrm{e}}(x,t)$	$\dfrac{\partial(\epsilon c_{\mathrm{e}})}{\partial t} = \dfrac{\partial}{\partial x}\left(D_{\mathrm{eff}}(c_{\mathrm{e}},T)\dfrac{\partial c_{\mathrm{e}}}{\partial x}\right) + \left(\dfrac{1-t^+}{F}\right) j_{\mathrm{tot}}$
$c_{\mathrm{a}}(x,r,t)$	$\dfrac{\partial c_{\mathrm{a}}}{\partial t} = \dfrac{1}{r^2}\dfrac{\partial}{\partial r}\left(D_{\pm}(T) r^2 \dfrac{\partial c_{\mathrm{a}}}{\partial r}\right)$
$c_{\mathrm{s}}(x,t)$	$\dfrac{\partial c_s}{\partial r} = -\dfrac{N_{\mathrm{int}}}{D_{\pm}(T)}$
j_{tot}	$j_{\mathrm{tot}} = F a_{\pm}\left(N_{\mathrm{int}} + \sum N_{\mathrm{sr}}\right)$
N_{int}	$N_{\mathrm{int}} = 2k_{\pm}(T)\sqrt{\dfrac{c_{\mathrm{e}}}{c_{\mathrm{eq}}}(c_{\mathrm{m}\pm} - c_{\mathrm{s}})c_{\mathrm{s}}}\sinh\left(\dfrac{F\eta}{2RT}\right)$
η	$\eta = \phi_{\mathrm{s}} - \phi_{\mathrm{e}} - U_{\pm}(c_{\mathrm{s}}) - \eta_{\mathrm{SEI}}$

Table S1: Equations of the Doyle-Fuller-Newman (DFN) model.

Other electrode parameters were taken from Tables VII and IX of Chen *et* al.[2] and are shown in Table S2. The solid-state diffusion coefficients $D_{\pm}$ deserve special attention because O'Kane *et* al.[1] identified D_{-} as a critical parameter for Li plating/stripping. Chen *et* al.[2] made detailed measurements of $D_{\pm}$ as functions of Li^+ concentration, but neither Chen *et* al.nor the authors of this work were able to implement this in PyBaMM. Instead, the negative electrode diffusivity D_{-} is treated as a function of temperature only.

The temperature-dependent parameters $D_{\pm}(c_{\mathrm{a}}^*, T)$ and $k_{\pm}(T)$ are assumed to have Arrhenius temperature dependence:

$$D_{\pm}(T) = D_{\pm}(T_{\mathrm{meas}})\exp\left(\frac{E_{D\pm}}{RT_{\mathrm{meas}}} - \frac{E_{D\pm}}{RT}\right) \tag{S1}$$

$$k_{\pm}(T) = k_{\pm}(T_{\mathrm{meas}})\exp\left(\frac{E_{k\pm}}{RT_{\mathrm{meas}}} - \frac{E_{k\pm}}{RT}\right), \tag{S2}$$

where $E_{D\pm}$ and $E_{k\pm}$ are activation energies and T_{meas} is the temperature at which detailed measurements were carried out, in this case 298.15 K (25 °C).

However, Chen *et* al.[2] did not report temperature-dependent diffusivity data. For the negative electrode, an Arrhenius temperature dependence is assumed; the activation energy 30300 J mol^{-1} is taken from Ecker *et* al.[3] and is within one significant figure of two other values

Symbol	Definition	- electrode	+ electrode
A	Total planar electrode area, m^2	0.1027	0.1027
$a_\pm$	Surface area to volume ratio, m^{-1}	3.84×10^5	3.82×10^5
$c_{m\pm}$	Maximum Li^+ concentration, mol m^{-3}	33133	63104
$c_{0\pm}$	Initial Li^+ concentration, mol m^{-3}	29866	17038
$D_\pm$	Li^+ diffusion coefficient at 25 °C, m^2 s^{-1}	3.3×10^{-14}	4×10^{-15}
$E_{D\pm}$	Activation energy for Li^+ diffusion, J mol^{-1}	30300[3]	25000[6]
$E_{k\pm}$	Activation energy for rate constant, J mol^{-1}	35000	17800
$k_\pm$	(De)intercalation rate constant at 25 °C, m s^{-1}	2.12×10^{-10}	1.12×10^{-9}
$r_\pm$	Electrode particle radius, m	5.86×10^{-6}	5.22×10^{-6}
$\delta_\pm$	Electrode thickness, m	8.52×10^{-5}	7.56×10^{-5}
ϵ_e	Electrolyte volume fraction	0.25	0.335
ϵ_a	Active material volume fraction	0.75	0.665
$\sigma_\pm$	Electrode conductivity, S m^{-1}	215	0.18

Table S2: Electrode parameters for the beginning of life model. All values taken from the final model values from Tables VII and IX in Chen *et* al.[2] unless otherwise specified.

reported in the literature [4, 5]. The authors are unaware of any temperature-dependent diffusivity data for NMC 811, but Cabañero *et* al.[6] reported an activation energy of 25000 J mol^{-1} for the similar NCA material, so this value is taken.

Electrolyte parameters

The effective conductivity $\kappa_{\text{eff}}(c_e, T)$ and diffusion coefficient $D_{\text{eff}}(c_e, T)$ of electrolyte occupying volume fraction ϵ are related to the corresponding values $\kappa(c_e, T)$ and $D_e(c_e, T)$ in pure electrolyte by

$$\kappa_{\text{eff}}(c_e, T) = \epsilon_e^{1.5}\kappa(c_e, T) \quad \text{and} \quad D_{\text{eff}}(c_e, T) = \epsilon_e^{1.5} D_e(c_e, T). \tag{S3}$$

Both $\kappa(c_e, T)$ and $D_e(c_e, T)$ have an Arrhenius temperature dependence:

$$\kappa(c_e, T) = \kappa(c_e, T_{\text{meas}}) \exp\left(\frac{E_\kappa}{RT_{\text{meas}}} - \frac{E_\kappa}{RT}\right) \tag{S4}$$

$$D_e(c_e, T) = D_e(c_e, T_{\text{meas}}) \exp\left(\frac{E_\kappa}{RT_{\text{meas}}} - \frac{E_\kappa}{RT}\right), \tag{S5}$$

where E_κ is the activation energy for both κ and D_e, T_{meas} is the temperature at which detailed measurements were carried out (in this case, 298.15 K), $\kappa(c_e, T_{\text{meas}})$ is a cubic polynomial [2]

$$\kappa(c_e, T_{\text{meas}}) = 1.297 \times 10^{-10} c_e^3 - 7.94 \times 10^{-5} c_e^{1.5} + 3.329 \times 10^{-3} c_e \tag{S6}$$

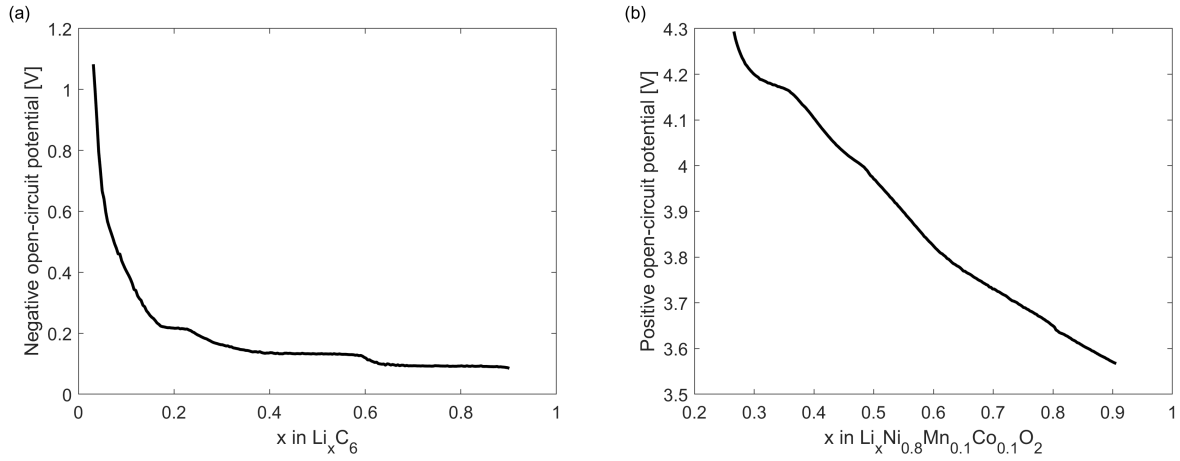

Figure S1: Open-circuit potential $U_{-}(c_{\mathrm{s}}^{*})$ of the (a) graphite+SiO_x negative electrode and (b) NMC 811 positive electrode, as a function of normalized Li^+ concentration, as measured by Chen *et* al.[2] at 25 °C.

and $D_{\mathrm{e}}(c_{\mathrm{e}}, T)$ is a quadratic polynomial [2]

$$D_{\mathrm{e}}(c_{\mathrm{e}}, T_{\mathrm{meas}}) = 8.794 \times 10^{-17} c_{\mathrm{e}}^2 - 3.972 \times 10^{-13} c_{\mathrm{e}} + 4.862 \times 10^{-10}. \tag{S7}$$

In (S6) and (S7), κ has units of S m^{-1}, $D_{\mathrm{e}}(c_{\mathrm{e}}, T)$ has units of m^2 s^{-1} and c_{e} has units of mol m^{-3}. The remaining parameters are taken from Table VII of Chen *et* al.[2] and listed in Table S3.

Degradation parameters

The parameters concerning battery degradation were not measured by Chen *et* al.[2]. The default degradation parameters in PyBaMM are taken from a range of sources and listed in Table S4. Some degradation parameters were varied as part of parametric studies and are assumed to have the values listed in Table S5 except in the study where that parameter is varied.

Two-layer diffusion-limited SEI growth model

In two-layer SEI models, the SEI thickness L_{SEI} is replaced with two thicknesses L_{inner} and L_{outer} for the inner and outer layers respectively. It is assumed that the solvent can only diffuse through the outer layer, so the boundary conditions on the solvent concentration c_{sol} become

$$N_{\mathrm{sol}} = -D_{\mathrm{sol}}(T) \frac{\partial c_{\mathrm{sol}}}{\partial l}, \tag{S8}$$

$$c_{\mathrm{sol}} = 0 \quad \text{at} \quad l = L_{\mathrm{inner}}, \tag{S9}$$

$$c_{\mathrm{sol}} = c_{\mathrm{sol},0} \quad \text{at} \quad l = L_{\mathrm{outer}}, \tag{S10}$$

Symbol	Definition	Value
c_{eq}	Equilibrium Li^+ concentration in electrolyte, mol m^{-3}	1000
E_κ	Activation energy for electrolyte conductivity, J mol^{-1}	17100[3]
F	Faraday's constant, C mol^{-1}	96485
Q_{nom}	Nominal capacity, mAh	5000
R	Universal gas constant, J K^{-1} mol^{-1}	8.314
t^+	Li^+ transference number	0.2594
V_{max}	Upper cutoff voltage, V	4.2
V_{min}	Lower cutoff voltage, V	2.5
δ_{s}	Separator thickness, m	1.2×10^{-5}
ϵ_{e}	Separator porosity	0.47

Table S3: Other parameters used in the model. All values taken from Chen *et* al.[2]

The solution is

$$c_{\mathrm{sol}} = \frac{l c_{\mathrm{sol},0}}{L_{\mathrm{outer}}}, \tag{S11}$$

$$N_{\mathrm{sol}} = -\frac{c_{\mathrm{sol},0} D_{\mathrm{sol}}(T)}{L_{\mathrm{outer}}}, \tag{S12}$$

$$N_{\mathrm{inner}} = -\tfrac{1}{2} N_{\mathrm{sol}} = \frac{c_{\mathrm{sol},0} D_{\mathrm{sol}}(T)}{L_{\mathrm{outer}}}, \tag{S13}$$

$$N_{\mathrm{outer}} = -\tfrac{1}{2} N_{\mathrm{sol}} = \frac{c_{\mathrm{sol},0} D_{\mathrm{sol}}(T)}{L_{\mathrm{outer}}}, \tag{S14}$$

$$\tag{S15}$$

assuming the two layers grow at the same rate. Two differential equations are required, one for each layer:

$$\frac{\partial L_{\mathrm{inner}}}{\partial t} = -\tfrac{1}{4} N_{\mathrm{sol}} \bar{V}_{\mathrm{SEI}} = \frac{c_{\mathrm{sol},0} D_{\mathrm{sol}}(T) \bar{V}_{\mathrm{SEI}}}{4 L_{\mathrm{outer}}}, \tag{S16}$$

$$\frac{\partial L_{\mathrm{outer}}}{\partial t} = -\tfrac{1}{4} N_{\mathrm{sol}} \bar{V}_{\mathrm{SEI}} = \frac{c_{\mathrm{sol},0} D_{\mathrm{sol}}(T) \bar{V}_{\mathrm{SEI}}}{4 L_{\mathrm{outer}}}. \tag{S17}$$

In all other equations, L_{SEI} can be substituted with $L_{\mathrm{inner}} + L_{\mathrm{outer}}$. For example:

$$\eta_{\mathrm{SEI}} = \rho_{\mathrm{SEI}} (L_{\mathrm{inner}} + L_{\mathrm{outer}}) \frac{j_{\mathrm{tot}}}{a_-}. \tag{S18}$$

References

[1] Simon E. J. O'Kane, Ian D. Campbell, Mohamed W. J. Marzook, Gregory J. Offer, and Monica Marinescu. Physical Origin of the Differential Voltage Minimum Associated with

Table S4: Degradation parameters used in the model, except for those that were varied during the parametric studies, which are given in Table S5.

		Negative electrode		Positive electrode	
Symbol	Definition	Value	Ref.	Value	Ref.
$c_{\text{sol},0}$	Bulk solvent concentration, mol m^{-3}	2636	[7]		
$\bar{V}_{\text{SEI}}$	SEI partial molar volume, m^3 mol^{-1}	9.585×10^{-5}	[8]		
ρ_{SEI}	SEI resistivity, Ω m	2×10^5	[8]		
$L_{\text{SEI},0}$	Initial SEI thickness, m	5×10^{-9}	[8]		
E_{sol}	Solvent diffusion activation energy, J mol^{-1}	37000	[9]		
$\alpha_{\text{a,Li}}$	Anodic transfer coefficient for Li stripping	0.35	Assumed		
$\alpha_{\text{c,Li}}$	Cathodic transfer coefficient for Li plating	0.65	Assumed		
E	Young's modulus [Pa]	1.5×10^{10}	[10]	3.75×10^{11}	[10]
ν	Poisson's ratio	0.3	[10]	0.2	[10]
Ω	Partial molar volume [m^3/mol]	3.1×10^{-6}	[10]	1.25×10^{-5}	[11]
$l_{\text{cr},0}$	Initial crack length [m]	2×10^{-5}	[12]	2×10^{-5}	[12]
w_{cr}	Initial crack width [m]	1.5×10^{-5}	[12]	1.5×10^{-5}	[12]
ρ_{cr}	number of cracks per unit area [m^{-2}]	3.18×10^{15}	[12]	3.18×10^{15}	[12]
b_{cr}	Stress intensity factor correction	1.12	[12]	1.12	[12]
m_{cr}	Paris' law exponential term	2.2	[12]	2.2	[12]
σ_{c}	Critical stress for particle fracture [Pa]	6×10^7	Assumed	3.75×10^8	Assumed
m_2	Loss of active material exponential term	2	Assumed	2	Assumed

Lithium Plating in Li-Ion Batteries. *Journal of The Electrochemical Society*, 167(9):090540, 2020.

[2] Chang-Hui Chen, Ferran Brosa Planella, Kieran O'Regan, Dominika Gastol, W. Dhammika Widanage, and Emma Kendrick. Development of Experimental Techniques for Parameterization of Multi-scale Lithium-ion Battery Models. *Journal of The Electrochemical Society*, 167(8):080534, 2020.

[3] Madeleine Ecker, Stefan Käbitz, Izaro Laresgoiti, and Dirk Uwe Sauer. Parameterization of a Physico-Chemical Model of a Lithium-Ion Battery. *Journal of The Electrochemical Society*, 162(9):A1849–A1857, 2015.

Table S5: Degradation parameters varied during the parametric studies, along with their default values.

		Negative electrode		Positive electrode	
Symbol	Definition	Default value	Ref.	Default value	Ref.
D_{sol}	Solvent diffusivity in SEI, $m^2\ s^{-1}$	2.5×10^{-22}	[13]		
k_{Li}	Li plating/stripping rate constant, $m\ s^{-1}$	10^{-9}	Assumed		
γ_0	Rate constant for dead Li formation, s^{-1}	10^{-6}	Assumed		
k_{cr}	Paris' law cracking rate	3.9×10^{-20}	[12]	3.9×10^{-20}	[12]
β	Loss of active material proportional term	0.001	Assumed	0.001	Assumed

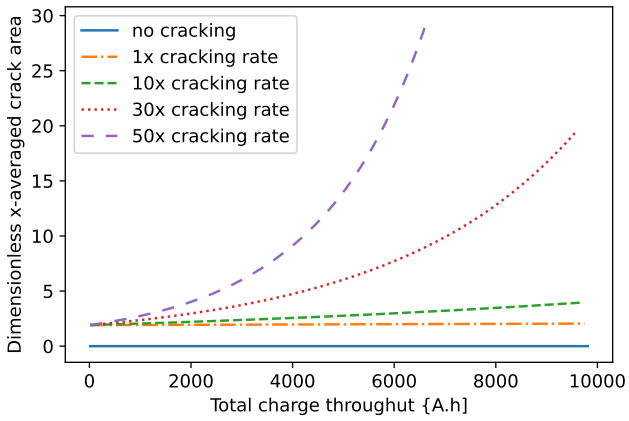

Figure S2: Increase in dimensionless crack area (interfacial area of cracks divided by interfacial area without cracks) during the parametric study for particle cracking.

[4] T. L. Kulova, A. M. Skundin, E. A. Nizhnikovskii, and A. V. Fesenko. Temperature effect on the lithium diffusion rate in graphite. *Russian Journal of Electrochemistry*, 42(3):259–262, 2006.

[5] Johannes Schmalstieg, Christiane Rahe, Madeleine Ecker, and Dirk Uwe Sauer. Full Cell Parameterization of a High-Power Lithium-Ion Battery for a Physico-Chemical Model: Part I. Physical and Electrochemical Parameters. *Journal of The Electrochemical Society*, 165(16):A3799–A3810, 2018.

[6] Maria Angeles Cabañero, Nicola Boaretto, Manuel Röder, Jana Müller, Josef Kallo, and Arnulf Latz. Direct determination of diffusion coefficients in commercial li-ion batteries. *Journal of The Electrochemical Society*, 165(5):A847–A855, 2018.

[7] Harry J. Ploehn, Premanand Ramadass, and Ralph E. White. Solvent Diffusion Model for Aging of Lithium-Ion Battery Cells. *Journal of The Electrochemical Society*, 151(3):A456, 2004.

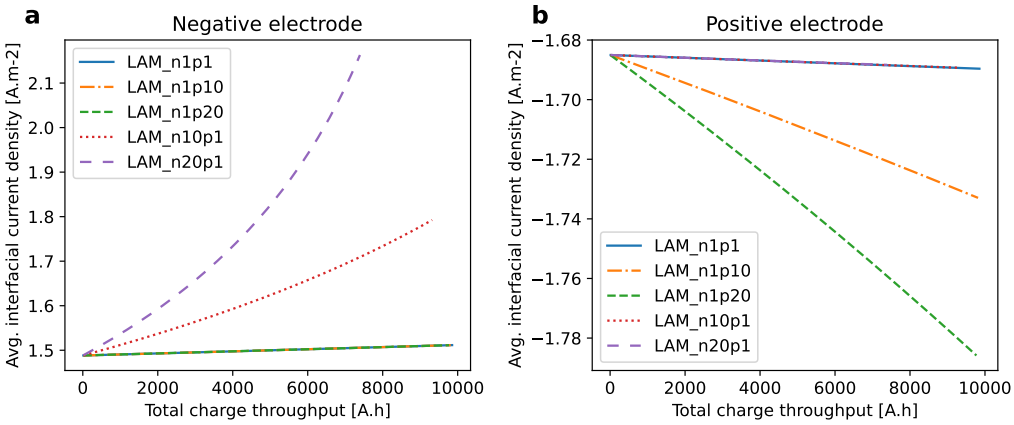

Figure S3: Influence of loss of active material on the magnitude of averaged interfacial current density during battery discharge in the: (a) negative electrode and (b) positive electrode.

[8] M. Safari, M. Morcrette, A. Teyssot, and C. Delacourt. Multimodal Physics-Based Aging Model for Life Prediction of Li-Ion Batteries. *Journal of The Electrochemical Society*, 156(3):A145, 2009.

[9] Thomas Waldmann, Marcel Wilka, Michael Kasper, Meike Fleischhammer, and Margret Wohlfahrt-Mehrens. Temperature dependent ageing mechanisms in lithium-ion batteries – a post-mortem study. *Journal of Power Sources*, 262:129–135, 2014.

[10] Weilong Ai, Ludwig Kraft, Johannes Sturm, Andreas Jossen, and Billy Wu. Electrochemical Thermal-Mechanical Modelling of Stress Inhomogeneity in Lithium-Ion Pouch Cells. *Journal of The Electrochemical Society*, 167(1):013512, 2020.

[11] Rong Xu, Yang Yang, Fei Yin, Pengfei Liu, Peter Cloetens, Yijin Liu, Feng Lin, and Kejie Zhao. Heterogeneous damage in Li-ion batteries: Experimental analysis and theoretical modeling. *Journal of the Mechanics and Physics of Solids*, 129(2019):160–183, 2019.

[12] Justin Purewal, John Wang, Jason Graetz, Souren Soukiazian, Harshad Tataria, and Mark W. Verbrugge. Degradation of lithium ion batteries employing graphite negatives and nickel-cobalt-manganese oxide + spinel manganese oxide positives: Part 2, chemical-mechanical degradation model. *Journal of Power Sources*, 272:1154–1161, 12 2014.

[13] Fabian Single, Arnulf Latz, and Birger Horstmann. Identifying the Mechanism of Continued Growth of the Solid–Electrolyte Interphase. *ChemSusChem*, 11(12):1950–1955, 2018.

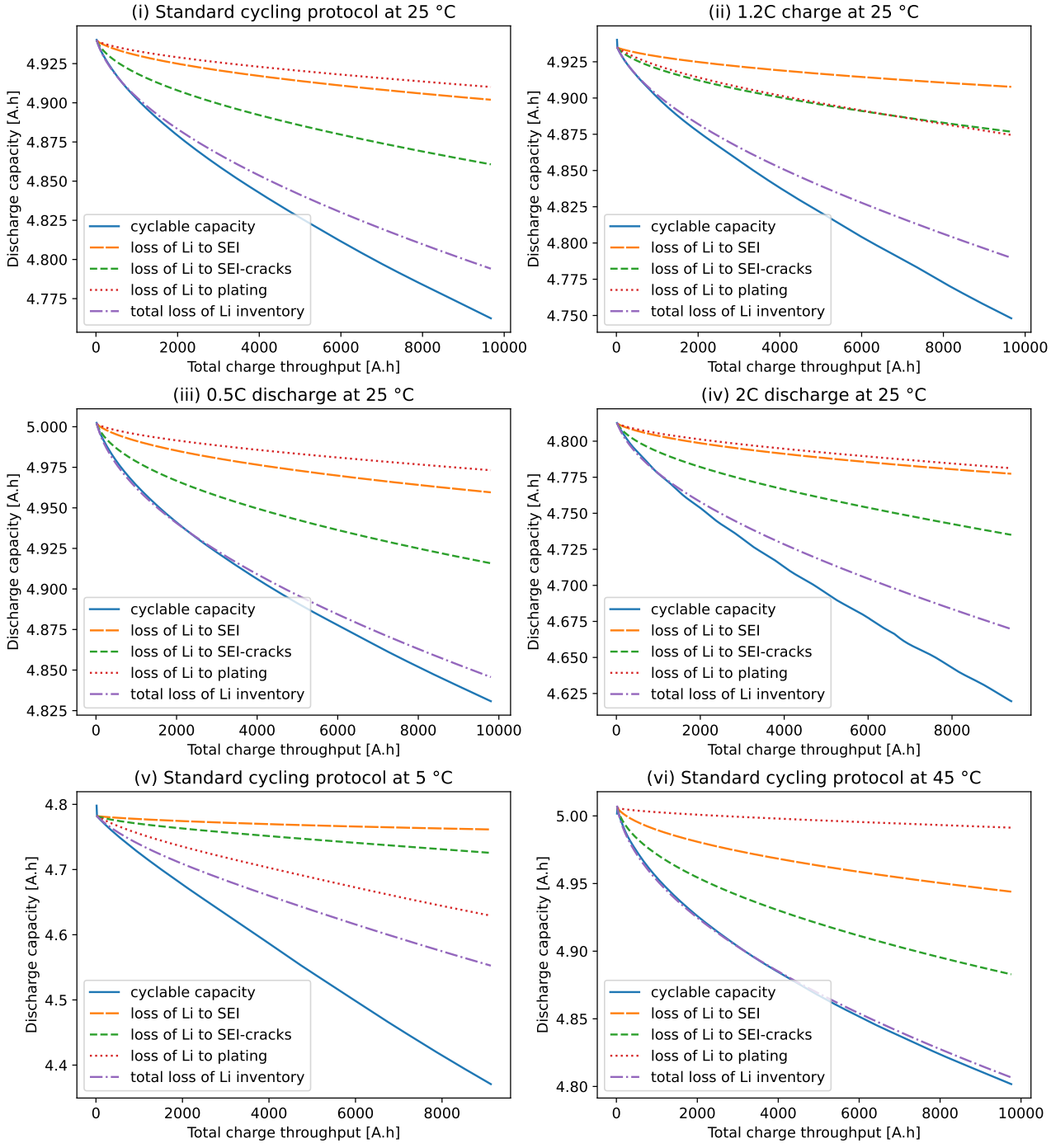

Figure S4: Loss of lithium inventory for cycling protocols (i)-(vi), with contributions from each mechanism: surface SEI, SEI on cracks and lithium plating. The cyclable capacity is also shown for comparison.